Citation: Lança M, Gomes J, Cabral D, Hosouli S., (2024) 'Thermal performance of three concentrating collectors with bifacial PV cells. Part II – parametrical study', *Proceedings of the Institution of Mechanical Engineers, Part A: Journal of Power and Energy*, 238(4), pp. 723-730. Copyright © 2024 IMechE. DOI: 10.1177/09576509241231852.

Thermal Performance of Three Concentrating Collectors with Bifacial PV Cells. Part II – Parametrical study

Miguel Lança[1], João Gomes[2,3], Diogo Cabral[2] and Sahand Hosouli[4]

[1] Instituto Superior Técnico, Lisbon University, Portugal

[2] Department of Building Engineering, Energy Systems and Sustainability Science, University of Gävle, Sweden

[3] MG Sustainable Engineering AB, Sweden

[4]Department of Mechanical Engineering, Kingston University, London, UK

[1]miguel.lanca@tecnico.ulisboa.pt

Abstract

One of the problems in using PV cells to extract energy from sunlight is the temperature effect on PV cells. As the solar panel is heated, the conversion efficiency of light to electrical energy is diminished. Moreover, successive temperature elevations can cause dilatations in the array of cells which may also contribute to the degradation of the receiver. Some of the operating temperature mitigation approaches may include air-flow ventilation. In this study, data obtained by experimental and numerical simulations of a collector with bifacial PV cells is compared to the expressions found in the literature for the estimation of the heat transfer coefficient. Forced ventilation was applied to the studied collector as it accounts for much better heat dissipation. A new correlation for the estimation of the heat transfer coefficient is developed for such a geometry, for inlet velocities ranging between 3 and 8 m/s. Values of heat transfer coefficient estimated in the present work have been compared with studies of other researchers.

Keywords: bifacial PV cells, concentrators, PV cooling, CFD, convection heat transfer

1. Introduction

Whereas thermal collectors may benefit from the insulation minimization of heat losses, PV

cells see their electric output diminished when operating temperatures arise. To achieve optimum temperatures, several techniques are used to enhance the productivity of the collector. Researchers have developed two primary techniques for cooling solar cells: active and passive systems. Proper cooling of PV modules reduces output loss and enhances their reliability. Active cooling uses coolants like water or air, driven by fans or pumps, while passive methods don't require additional energy for cooling. There's significant research on utilizing various coolants, such as water or glycols, to manage temperature, with economic considerations assessing if the power gains offset the consumption. Passive cooling is segmented into air, water, and conductive cooling, often integrating components like heat sinks or exchangers for effective natural convection. Heat sinks, made from materials with high thermal conductivity, are placed underneath solar panels to efficiently dissipate heat. Given their simplicity and cost-effectiveness, passive techniques are favored. As cooling tech has advanced, it now incorporates elements like heat exchangers, nanofluids, and thermoelectric generators. An emerging area focuses on beam-splitting technology, segregating wavelengths for PV cells from those used in combined photovoltaic-thermal systems ([1]).

[2] tested a solar air heater with its absorber plate roughened with V-shaped ribs. Forced cooling was added to the collector utilizing a blower. It is found that the maximum heat transfer occurs in the vicinity of the re-attachment point. It is also found that the roughness pitch ratio of 10 yields the best performance.

[3] studied theoretically a strategy for the cooling of PV cells using ducts. It is reported that the temperature rise of the cells is minimized when the ratio L/D of the duct (its length to its hydraulic diameter) is around 20. It is also shown that the optimum proportion is practically independent of the slope of the array of cells.

[4] have shown experimentally that the differences between heat transfer in air solar collectors compared to other types of collectors are because: 1 - the upper and lower walls of the solar collector's channel are different in the two cases and 2 - there is a large turbulence intensity at the inlet of the channel, which is damped not only by the thickness of the sublayer, but also by the length direction of the channel. Inlet Reynolds number was found to be approximately 10^4 in their experiments.

Various cooling methods have been proposed by [5], for the cell´s cooling. A bare solar panel with no air velocity was used as a base model. This was tested and compared to bare solar panels cooled by heat sinks, in the form of extended surfaces such as plate fins that can be mounted on the back surface of solar panels. Results showed that the heat sinks were only

marginally effective as they resulted in a steady-state temperature of only a few degrees less than a solar panel without a heat sink.

In a study by [6], various cooling techniques for PV modules were examined, emphasizing the radiative cooling method. Elevated temperatures can degrade PV modules' efficiency and reliability. While many cooling methods exist, the radiative cooling method, a passive technique, was highlighted. However, their research revealed that modifications to surface emissivity had minimal impact on cooling when compared to conventional methods, with a mere ~1°C temperature reduction. Thus, while radiative cooling is promising, it currently lacks the effectiveness of other established cooling strategies, emphasizing the need for continued research in this area.

Various liquid-based cooling methods have been assessed for enhancing the efficiency of PV modules. While the forced water circulation technique shows promise in terms of efficiency, its practicality is offset by the high costs, making it less suited for expansive solar farms. Similarly, the liquid immersion cooling technique, highlighted by a study from [7], demonstrated a significant 17.8% boost in efficiency when PV modules were submerged. However, its feasibility becomes limited for applications like floating solar systems. On the other hand, the water spraying approach can increase efficiency by up to 15%, but its viability is questioned due to its substantial water usage. In this case balancing the efficiency gains with practical and environmental concerns is pivotal in determining the optimal cooling strategy [1].

[8] have worked to enhance and improve the electrical output efficiency of common silicon-based solar PV modules by lowering their operating temperature. This was accomplished by attaching hollow rectangular aluminum tubes as a fin to the rear surface of the solar PV panel. The proposed geometrical configuration of tubes helped to increase the heat transfer rate to the surrounding air by increasing the effective area without increasing the overall weight of the collector. A comparative analysis has also been presented for PV modules with and without fins. The cooling effect produced due to fins improved the open-circuit voltage up to 12.97 % and electrical output efficiency up to 2.08 %.

According to a review in the performance improvement for building integrated photovoltaics, estimations through computational fluid dynamics and experimental tests, show a maximum reduction of 20 º C in cell temperature which can be achieved just by promoting natural air flow. This can be attained by creating a gap between the panels and the rooftop, ([9]). According to the same study, power output was increased by 19% when forced ventilation was applied, after deducting the electricity used to power the fans.

In a more recent study conducted by [10], the performance of solar panels was significantly enhanced using a hybrid cooling system that combined thermoelectric coolers (TECs) and phase change materials (PCMs). Their simulations revealed an optimal combination of Vaseline as the PCM with Silver as the back casing, leading to a 9.7% increase in panel efficiency. However, practical experiments with copper, chosen for economic reasons, also yielded a noteworthy efficiency increase of 9.56%. Most strikingly, their Hybrid Cooling Technique, an innovative amalgamation of TECs, PCMs, and Aluminum Heat Sinks, resulted in a substantial 19.4% increment in electrical efficiency and 19.32% in panel efficiency.

The use of PV cells is gaining significant traction globally, with an emphasis on maximizing the energy extracted from sunlight. However, as PV cells operate, they are susceptible to temperature fluctuations which can compromise their efficiency, and even longevity. Elevated temperatures not only decrease the conversion efficacy from light to electricity, but successive temperature rises can degrade the receiver. Previous research has approached this issue with varying cooling strategies, such as duct cooling, natural airflow, and the use of heat sinks. Yet, despite these advances, a coherent understanding of the intricacies of PV cell temperature management, especially in the context of forced ventilation, remains somewhat elusive. There's an undeniable need to investigate and establish more effective cooling mechanisms, quantify heat transfer efficiencies, and provide designers with reliable data and equations for better PV cell designs. Our study, through both experimental and numerical means, seeks to bridge this knowledge gap, offer a new perspective on the heat transfer coefficient, and contribute to the evolution of PV cell temperature management techniques. This paper makes use of a previously validated CFD model, for the investigation of the effect the velocity of the air has on the heat transfer coefficient of the receiver of a concentrated PV collector. Predicted heat transfer coefficients are compared to the expressions used in literature when estimating heat losses in collectors and a new equation is proposed which hopefully can be used in the design of collectors. This endeavor not only aligns with the growing demand for sustainable energy solutions but also fosters the potential for more effective, durable, and efficient PV cell applications.

This study aims to compare the performance of a previous numerically modeled PV cooling strategy. Since the variation of the inlet velocity of the cool air which strikes the collector is known to increase turbulence and thus the heat transfer between the PV cells and the fluid, a parametric study is carried out in this article to analyze the cooling potential of this strategy. A more practical contribution of this study is to come up with a new empirical expression which can be used by technicians and thermal systems designers to estimate the heat transfer

coefficient when forced ventilation is applied specifically to a CPC PV collector.

2. Methodology

A CFD model is used so that a parametric study could be carried out when investigating the performance of a new method for PV cells cooling. To validate the numerical results, a set of reliable and high-quality experimental data was necessary. The CFD model used here is the same one used in the first part of this study, which has already been validated by experimental results [18]. In [18] three collectors were tested and simulated numerically - Case 1 corresponds to the collector tested which is hermetically closed. Cases 2 and 3 were considered prototypes since they represent new collectors which haven´t been tested experimentally. In case 2 the lateral gables have been removed so the cooling relies only in natural ventilation, and in case 3 a pair of fans were installed in one of the gables of the collector. Reduction of 13.5 % in temperature of the PV cell surface is found when comparing case 1, a completely airtight collector, equipped with glass and side covers, with case 2 - without the side gables. Compared to natural convection mechanisms, forced convection results in an increased cooling effect. A reduction of 22.8% was found in the maximum operating cell temperature comparing the case 1 and 3.

The model used in the Part I of this study will serve as a reference for the present article – Part II, either for validation and parametrical study purposes.

2.1. Experimental set-up

Several tests have been performed on a CPC collector equipped with bifacial PV cells as shown in Fig. 1. The experimental set-up is described more in detail in the first part of this study. Thus, a briefer description is found in this section.

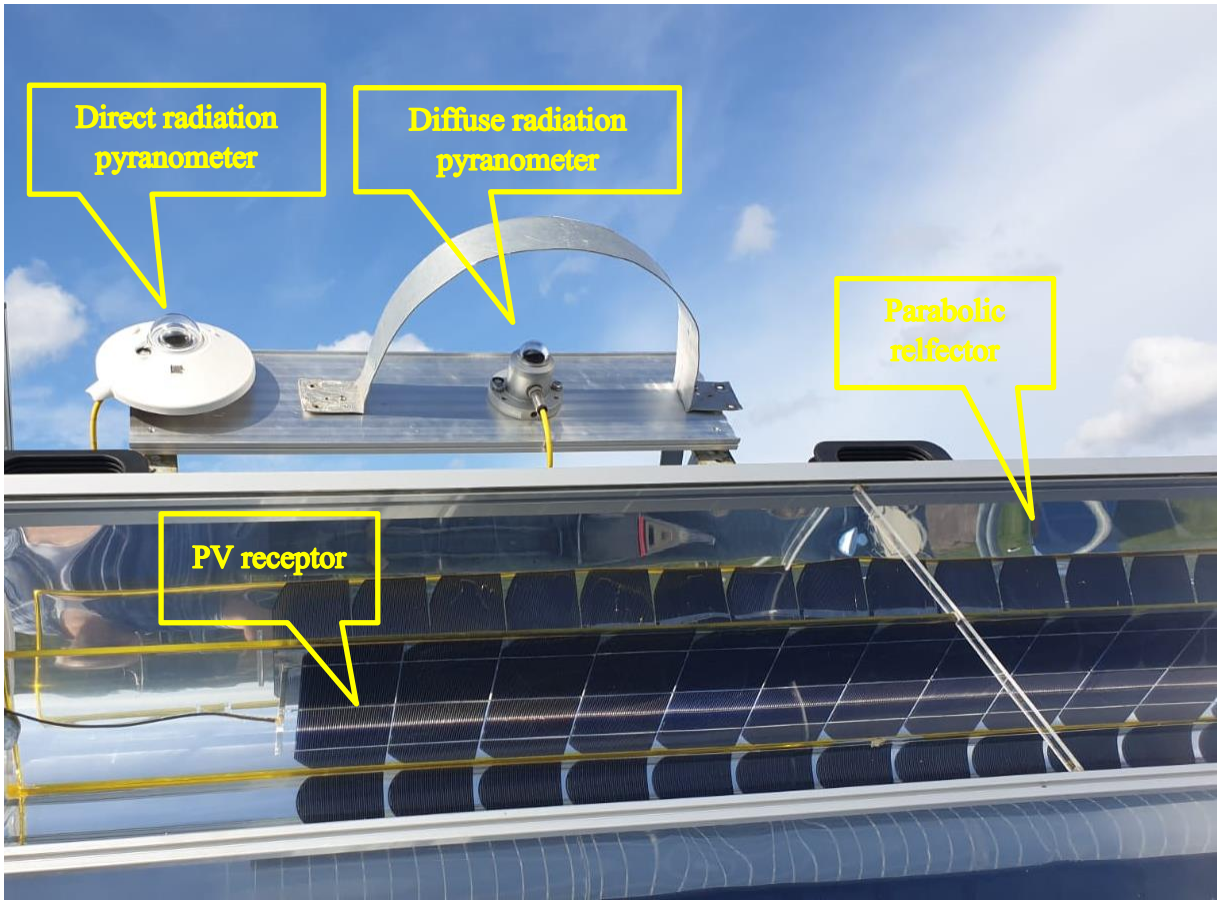

Figure 1: Detail of the collector tested experimentally

Two K-type thermocouples coded as *TC1* and *TC2* have been placed to measure the air and cell temperature, respectively and connected to a data-logger. A hot wire anemometer and two pyranometers have also been used.

2.1.1 Experimental procedure

The CPV solar collector was installed on a solar collector stand at the University of Gävle laboratory in Sweden and the outdoor testing procedure has been performed. As instantaneous readings were recorded, time was given for the readings to stabilize. The outdoor measurements were recorded from 11 a.m. and 1 p.m as the projected solar altitude is fairly constant throughout this period. Readings were taken every 30 minutes. The time interval was chosen to give the collector enough time for the temperature to stabilize. Global and diffuse solar radiation was measured and stored by two pyranometers located in the same collector plane.

2.2. Mathematical and numerical models

A commercial CFD code by Ansys-Fluent (release 17.0) has been used in this study, to predict the temperature and heat transfer coefficient in the PV cells. The first part of the study focuses

on the presentation of experimental results which served as means for the validation of the CFD code. For that purpose, a standard case of an air-tight collector, coded as case 1, was utilized. Then, a second and a third case made use of the same CFD model, already validated, in order to investigate a more efficient method for PV cell cooling. In this part of the study, only the third case is the model elected for this parametric study. In this model a pair of fans are attached to one of the gables to promote the airflow inside the collector. The inlet velocity is the parameter to vary and the heat transfer coefficient the main parameter to be analyzed. Besides the velocity of 5 m/s considered in the first part of this study, other 5 velocities are considered in the following sections. The following Fig. 2 shows a heat flow network used to describe the thermal analysis used in the study.

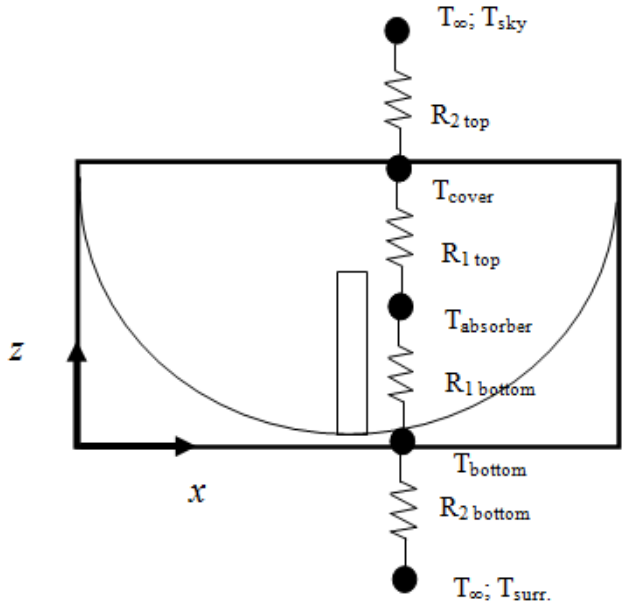

Figure 2: Equivalent heat flow network for the covered collector.

To ease the investigation, the following assumptions were made: 1) The system is in a quasi-steady state; 2) The heat capacity of the PV module, enclosed air, glass cover and reflector is negligible; 3) All thermal properties except air density are considered constant. The overall energy balance for the transient state is given by eq. 1.

$$G_{collector} A_{absorber} \tau_{cover} \alpha_{absorber} = q_{loss} + \frac{de_{collector}}{dt} \qquad \text{(eq. 1)}$$

Where $G_{collector}$ is the solar irradiation striking the collector, $A_{absorber}$ is the area of the collector, τ_{cover} is the glass transmittance and $\alpha_{absorber}$ the receiver absorptance. q_{loss} represents the heat loss due to conduction, convection and radiation and $\frac{de_{collector}}{dt}$ denotes the transient term. Assuming steady-state and one-dimensional heat analysis, q_{loss} can be calculated as follows:

$$q_{loss} = \frac{T_{absorber} - T_{\infty}}{R_{total}} \quad \text{(eq. 2)}$$

And each of the convection/radiation combined resistance components can be expressed by equation 3:

$$R_{total} = \frac{1}{R_{1top}} + \frac{1}{R_{2top}} + \frac{1}{R_{1bottom}} + \frac{1}{R_{2bottom}} \quad \text{(eq. 3)}$$

Where R_{1top} is a parallel resistance electric analog circuit, consisting of the convection and radiating components, taking place between the receiver and the cavity, and R_{2top} represents the combination between the two resistances that form the radiating and convective heat transfer between the glass and the exterior medium. The same principle is applied to the bottom, where $R_{1bottom}$ and $R_{2bottom}$ designate the resistances represented by the collector bottom surface (i.e. reflector outer surface) – convection and radiation, respectively, between the receiver and the cavity and the outer case, with the environment. The heat resistance due to convection R_{1top} is the key parameter geometry and cooling mechanism considered in this study which has to be evaluated separately, depending on the velocity magnitude induced by the forced ventilation.

2.3. Convection coefficient correlations

This paper conducted a parametric study for the evaluation of a cooling strategy proposed to enhance the operating conditions of the cells and presumably to increase the annual production of electricity of a CPV collector. From a collector design point of view, authors consider useful to bring to the analysis a comparison between the results obtained by the CFD calculations with some of the expressions encountered in literature for the calculation of the heat transfer coefficient in a collector. Due to their practicality these are often employed when designing collectors.

A widely used expression for the calculation of heat losses between the cover glass and the environment is given by [11]:

$$h = 2.8 + 3 \times V_{wind} \quad \text{(eq. 4)}$$

where V_{wind} is the wind speed. This expression accounts for the convective heat transfer only. The convective heat transfer between the cover glass and ambient can be approximated to the physics involved in the convection in flat plates. Other studies related to the heat transfer in rooms and buildings also use the expressions derived from flat plates heat transfer theory. This is because interior surfaces like walls and ceilings have losses to the conditioned supplied air. Therefore, in these situations, spaces can be considered as having a homogeneous distribution of temperature and their surfaces treated as flat plates. Heat transfer coefficient is therefore sometimes necessary for the estimation of building heat losses and gains. [12] proposes the following expression for the calculation of the heat transfer coefficient in walls:

$$h = 6.1\left(\frac{V^4}{H}\right)^{\frac{1}{5}} \qquad \text{(eq. 5)}$$

where V is the air supply velocity that is leaving the ventilation device and H a characteristic length.

The results given by equations 4 and 5 will be analyzed in this study and compared with the results from CFD predictions. That is to say that in equations 4 and 5, the input variable V will be the inlet velocity used in the simulations and H is the receiver length.

2.4. The CFD model

The commercial code Ansys-Fluent, release 17.0, was used in this study to predict the temperature distribution and the heat transfer coefficient in a CPC PV collector. The model used in the simulations is shown in Fig. 3.

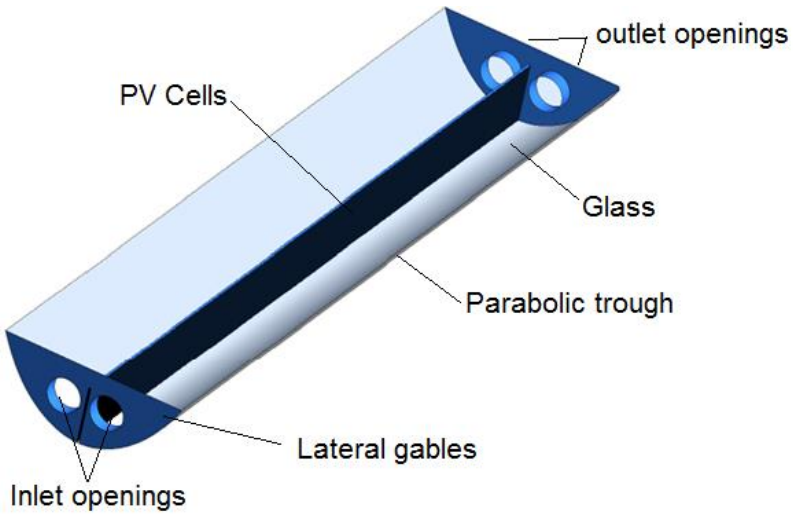

Figure 3: Model of the concentrating collector studied.

2.4.1. Setup

2.4.1.1. Turbulence

The standard k-ε turbulence model has been widely used in fluid flows with and without heat transfer because it combines relatively good accuracy and robustness of results within a wide range of applications without compromising the calculation time. It is a semi-empirical model of two equations in which the turbulent transport variables are the turbulent kinetic energy (k) and the dissipation rate (ε). In this study, the standard model was used due to the good performance achieved in similar applications ([13]), and the default constants were left unchanged.

Enhanced wall treatment has been employed in this study. It comprises a two-layer model ([14]) in which the transition between the zones is made by applying a blending function ([15]).

2.4.1.2. Boundary conditions

The boundary conditions were defined to describe appropriately the physical conditions depending on the collector component surface: a wall-type, velocity inlet-type and pressure outlet-type. Each boundary condition is defined in Table 1 and Table 2 for the momentum and energy respectively.

Table 1: List of boundary conditions assigned to each surface of the prototypes for the momentum equation.

***EWT* and *n.a.* stands for Enhanced Wall Treatment and not applicable, respectively.**

	Type of boundary condition for the momentum equation
Glass – exterior surface	n.a.
Glass – interior surface	EWT
Reflector – exterior surface	n.a.
Reflector – interior surface	EWT
Gables – interior surface	EWT
Receiver	EWT
Gables – exterior surface	n.a.
Air inlet	velocity inlet (in the range of 3-8 m/s)
Air outlet	pressure outlet (0 Pa)

Table 2 - List of boundary conditions assigned to each surface of the prototypes for the energy equation. *EWT* stands for Enhanced Wall Treatment. [1]The solar heat flux input equals 990 W/m^2 direct and 105 W/m^2 diffuse.

	Type of boundary condition for the energy equation
Glass – exterior surface	prescribed solar heat flux[1] convection+radiation
Glass – interior surface	EWT
Reflector – exterior surface	convection+radiation
Reflector – interior surface	convection+radiation
Gables – interior surface	convection+radiation
Gables – exterior surface	convection+radiation
Receiver	convection+radiation
Air inlet	prescribed temperature (29°C)
Air outlet	prescribed temperature (29°C)

The "pressure outlet" boundary condition type was chosen (with gauge pressure taken equal to zero) to define the static pressure at the flow outlets. In this case, backflow total temperature is taken equal to ambient temperature, which was considered constant over time. The "wall" boundary condition type is used to define the fluid-solid interface. The remaining external walls were defined considering losses by convection and radiation. Convection boundary condition type implies the definition of a medium temperature and an external convection coefficient. In the case of the glass surface, the latter was calculated by the expression given in [16], considering 2 m/s for the wind speed. In the case of the bottom of the collector as well as the gables, this coefficient was determined analytically using expressions for the heat transfer in flat plates ([17]).

2.4.1.3. Radiation

The radiation emitted by the bodies will be absorbed by the surrounding surfaces conditioning the final balance of energy.

The Solar Model

Ansys-Fluent provides a solar load model that can be used to calculate radiation effects from the sun's rays that enter a computational domain. The simulations were carried out using

Discrete Ordinates radiation model. Inputs of 990 W/m^2 of direct radiation, as well as 105 W/m^2 of diffuse radiation, were considered. The sun direction vector was taken as pointing over z-axis only. Therefore, the model assumes the incident solar radiation is striking the collector perpendicularly (i.e. at normal incidence).

2.4.2. Grid generation

The geometric model used in the CFD simulations was a simplified representation of the reduced scale test facility. The computational domain includes the space occupied by the air, and the interior of the receiver, which is assumed to be homogeneous. A mesh was created on solid domains to enable the heat conduction calculation by Ansys-Fluent software. The mesh size and also the results of using coarser or finer meshes can be found more in detail in the first part of this study.

2.4.3. Numerical solution algorithm

The finite volume method was used to solve the governing equations. The discretization of the convective terms of the momentum, energy and turbulence equations was done using the second-order upwind numerical scheme. The solver was set to steady-state and pressure-based type. The pressure-velocity coupling was determined by the SIMPLE algorithm. A convergence criterion relied on the magnitude of the unscaled residuals. A threshold of 10^{-3} is used for the residuals of continuity, momentum and turbulence, and 10^{-6} for the energy and radiation equations together with the monitoring of the temperature integral over a plane. This way more than one indicator is used over the iteration process when judging convergence of the solution. This approach implies that both the magnitude of the residuals and the temperature integral monitor are taken into account when judging the convergence of the solution.

2.4.4. Solver settings

The 3-D model was incorporated on Ansys-Fluent software (release 17.0), and momentum, energy, radiation, and turbulence equations were calculated. The solver general settings were defined as an incompressible steady regime. The discretization of the momentum, energy and turbulence equations followed a second-order upwind type numerical scheme.

3. Results and discussion

3.1. Parametric study

3.1.1. The influence of the inlet air speed in the temperature of the collector

In this section, the effect of different air inlet velocities is investigated on the temperature of the receiver of the collector. This analysis will make use of the CFD model previously described and already validated in the first part of this study. Six levels of velocity are considered, two of which are below the velocity of 5 m/s and three above. This is a sufficiently wide range for results to be analysed and at the same time, this variation would be easily achieved in practice through the installation of a pair of small ventilators equipped with speed control. The range of air velocity in the inlet was varied from 3 to 8 m/s. The results of applying the original velocity of 5 m/s are also shown here for benchmark purposes.

Figure 4 shows the calculated temperatures obtained along a line located in the surface of the receiver for 6 different inlet air velocities. This a centreline drawn from a point of the surface receiver close to the air inlet all way to a point close to the air outlet and it is equivalent of line *HC1* used in the previous analysis (see the first part of this study).

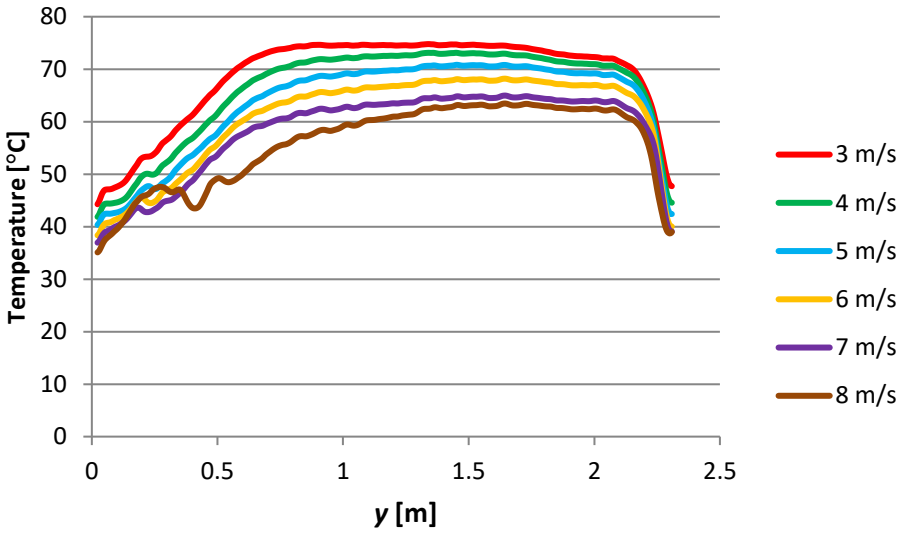

Figure 4 – Calculated temperature profiles over a line located in the cell surface for six air velocities in the inlet.

Results show a direct relation between the maximum temperatures reached by the receiver with the velocity of the air in the inlet, as expected. Higher velocities clearly denote lower temperatures of cells wherever the position being analysed. An exception of this is detected for the simulation with 8 m/s namely in the first 200 mm of the receiver. This is probably because of the momentum attained by the jet because of a higher velocity being employed, which results

in a more effective decrease in the receiver temperature a little farther, compared to the simulations for 6 and 7 m/s velocities.

Figure 4 points out also a more abrupt increase in the temperature for lower velocities than the opposite. As a result, the receiver temperature distribution varies between each velocity. If we consider the extremes and take the minimum and maximum velocities, for example, the maximum temperature is reached at y=0.78 m and y=1.64 m respectively.

3.1.2. The influence of the inlet air velocity in the heat transfer coefficient of the receiver

Besides the analysis of the temperature encountered on the cells for several velocities, it would be also interesting to investigate the effectiveness of the cell cooling mechanism using a variable of the amount of heat transferred to the air. The quantification and analysis of the convective heat transfer coefficient are addressed in this section to accomplish this goal.

Fluent computes the heat transfer coefficient through the solid/fluid interface using the reference temperature, heat flux and fluid velocity and its properties. Even though the reference temperature adopted may be subjective and lead to disparity of results, it should constitute a reliable and consistent method when comparing the thermal performance for each one of the 6 velocities, since the methodology of calculus is the same for every simulation. When the CFD code is asked to compute the heat transfer coefficient over a surface, the software displays the calculated contours in each one of the control volumes of the surface of the receiver. Post-processing of the results may be displayed graphically or, if desired, on a chart. The latter often yield a cloud of points since the variable is calculated for every volume control. For that reason and in order to get a more concise and clear presentation of the heat transfer coefficient, a statistical analysis of the calculated data is proposed in this study instead of the cloud of points. This is because it is sometimes difficult to find a tendency or pattern in these raw data charts. At the same time, it allows the comparison between performances of each case. The proposed statistical approach will consist of taking the local convective heat transfer coefficient, calculated by the CFD code for every control volume, along *y*-direction, and apply an 80-period moving average to that data. This period was specifically elected in order to smooth out the noise and disparity of results without having too much lag i.e. being capable of capture sudden local variations. This average was calculated along with the control volumes that comprise the total domain of the receiver. The definition of a moving average, h'_y, used to draw the curve of Fig. 5 is given in equation 6.

$$h_y^{'} = \frac{h_{CV1} + h_{CV2} + \cdots + h_{CV80}}{80} \qquad \text{(eq. 6)}$$

In this expression h_{cv} is the wall heat transfer coefficient computed by Fluent in a particular control volume. Figure 5 clearly points out the direct relation between the velocity and the heat transfer coefficient. It can also be stated, by the analysis of Fig. 3 and Fig. 4, that greater velocities at the inlet lead simultaneously to higher heat transfer coefficients and lower temperatures of the receiver.

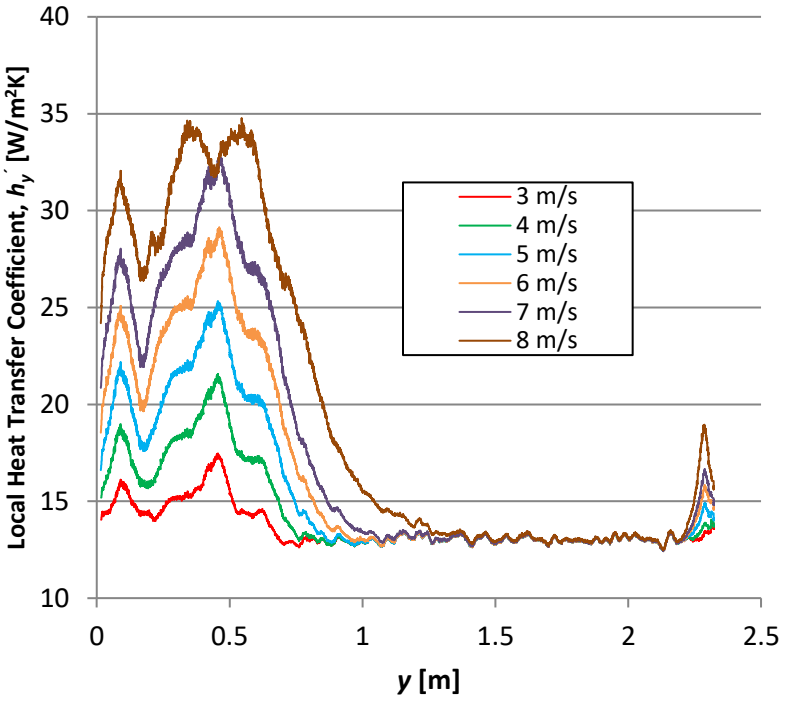

Figure 5 –Modified local heat transfer coefficient, $h_y^{'}$ shown as an 80 period moving average.

The results of the heat transfer coeficient yielded by equation 4 and equation 5 are compared with the simulated heat transfer coefficients. These will include every velocity considered in the discussion previously taken.

The predicted heat transfer coeficient varies considerably along the surface, as seen in Fig. 5. For that reason, an average value will be considered to be representative of a global value for comparisson purposes between equation 4, 5 and the calculations. The average heat transfer coefficient is calculated as follows:

$$\bar{h} = \left(\frac{\sum_{i=L_1-0.025}^{L_1+0.025} h_i}{10} + \frac{\sum_{i=L_2-0.025}^{L_2+0.025} h_i}{10} + \frac{\sum_{i=L_3-0.025}^{L_3+0.025} h_i}{10} + \frac{\sum_{i=L_4-0.025}^{L_4+0.025} h_i}{10} \right) \Big/ 4 \qquad \text{(eq.7)}$$

Where h_i is the heat transfer coefficient taken from the simulation in 4 positions of the receiver in *y*-direction: L_1=0.1 m; L_2=0.2 m; L_3=1 m and L_4=2 m. Data was picked up in 10 volume controls around the four positions, along the *y*-direction (25 mm for each side), the position L_i being placed in the center of those 10 measurements. Results were then averaged. Figure 6 summarizes the average heat transfer coefficient in the receiver for six inlet velocities according to equations 4, 5 and CFD.

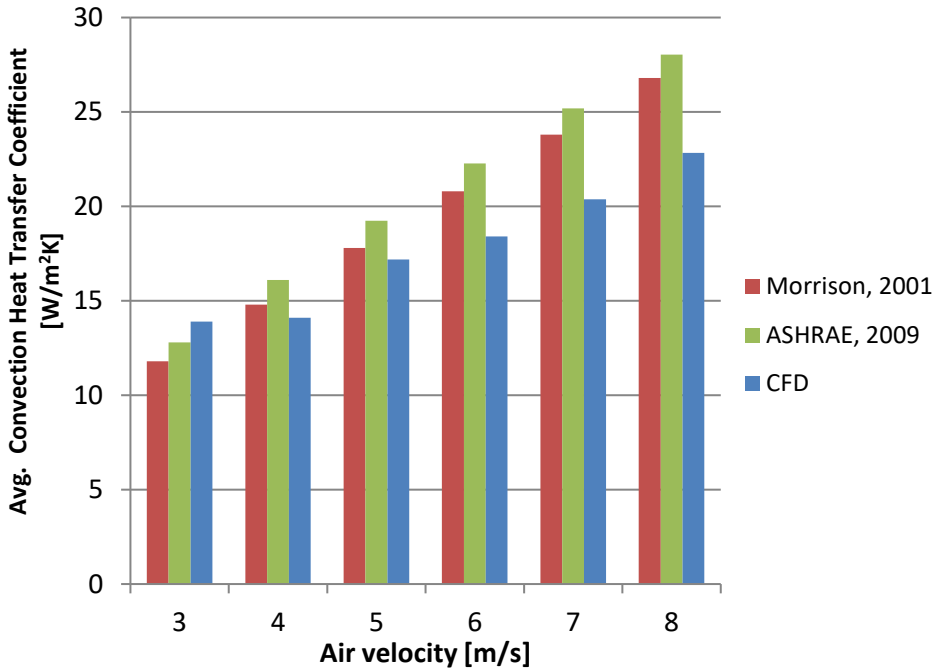

Figure 6 - Average heat transfer coefficient, $\bar{h}$, between the cell and the air for six air velocities in the inlet.

Overall, a good consistency is found between the results of the three methods. The ASHRAE, 2009 equation yields normally higher values than the Morrison, 2001 expression, while simulation results are generally the lowest of the presented data. Only for 3 m/s of air velocity, a higher figure is reported in CFD calculations. It is also visible an increasing discrepancy in the heat transfer coefficients yielded by each method with the increase of the velocities, namely when comparing CFD model and ASHRAE expression. The difference is about 20% less for the former.

In this study a new expression is proposed for the calculation of the heat transfer coefficient of ventilated thermal collectors. It was found by using a curve fit method applied to the results obtained in simulations and it is given by the following expression:

$$\bar{h} = 1.848 \times V_{inlet} + 11.33 \qquad \text{(eq. 8)}$$

Where V_{inlet} is the inlet air velocity induced by the ventilation system. The R-value associated with the linear regression is 0.971.

A numerical model was used in this study for the evaluation of the performance of a cooling system of PV cells. A new expression is produced from the simulations carried out on a previously validated CFD model. This expression can hopefully contribute to a better understanding of the physics involved in the mechanical cooling of a concentrating PV collector.

4. Conclusion

In the present article, a CFD analysis was performed to check the heat transfer capability of a new system designed for lowering the operating temperature of PV cells. This goal was achieved by the quantification of the heat transfer coefficient. This variable was obtained numerically by a validated CFD code. Some conclusions can be drawn about the results achieved here:

i) Compared to natural convection mechanisms, forced convection results in an increased cooling effect when applied to the collector.

ii) Higher airflow rates were reported to cause both an increase in the heat transfer coefficient and a decrease in the cell temperature. Comparing the lowest and highest velocities used in this study (3 and 8 m/s respectively), the heat transfer coefficient suffers an increment of 200%, whereas the maximum temperature of cells drops 14.8%.

iii) A new empirical correlation is provided for the calculation of the heat transfer coefficient when forced ventilation is applied to cool down PV collectors using CPC design and shows a good degree of fitting to the numerical results.

Besides the overall enhancement in the heat removal from the PV cells, it would be interesting to see how does this strategy compares to the different positioning of openings other than the ones considered in this study. Also, the number of fans used to cool down the cells, and the path followed by the air would have to be studied and/or optimized. The results and conclusion of this study may provide the designers with a new expression for estimating heat losses in a ventilated CPC-PV collector. These would hopefully aid the technician when choosing from different cooling systems of PV cells.

ACKNOWLEDGEMENTS

The authors would like to thank Gävle University, the company Solarus AB and Erasmus for the opportunity given to conduct the experiments that lead to the production of this article.

References

[1] Dwivedi, P., Sudhakar, K., Soni et al. Advanced cooling techniques of PV modules: A state of art. *Case studies in thermal engineering* 2020; 21: 100674.

[2] Dawagreh A, Momin A, Alkhasawneh H. Enhanced heat transfer in solar air heaters. *Asian Journal of Microbiology, Biotechnology and Environmental Sciences* 2018; 20. 843-847.

[3] Brinkworth BJ. Optimum depth for PV cooling ducts. *Solar Energy* 2006; 80(9):1131–4.

[4] Nassar Y, Sergievsky E. Heat transfer in flat-plate solar air-heating collectors. *Computational Studies* 2000; 3 pp. 575-584.

[5] Khatri A, Tenguria N. Enhancement of the efficiency of solar PV by increasing rate of heat transfer. *Smart Moves Journal IJOscience* 2019; Vol.5 No. 6, pp 10.

[6] Sato D, Yamada N. Review of photovoltaic module cooling methods and performance evaluation of the radiative cooling method. *Renewable and Sustainable Energy Reviews* 2019; 104, 151-166.

[7] Mehrotra S, Rawat P, Debbarma M et al. Performance of a solar panel with water immersion cooling technique. *International Journal of Science, Environment and Technology* 2014; *3*(3), 1161-1172.

[8] Khan S, Waqas A, Ahmad N et al. Thermal management of solar PV module by using hollow rectangular aluminum fins. *Journal of Renewable and Sustainable Energy* 2020; Nov 1;12(6).

[9] Dai Y, Bai Y. Performance Improvement for Building Integrated Photovoltaics in Practice: A Review. *Energies* 2020; 14(1):178.

[10] Singh D, Chaubey H, Parvez Y et al. Performance improvement of solar PV module through hybrid cooling system with thermoelectric coolers and phase change material. *Solar Energy* 2022; 241, 538-552.

[11] Morrison G. *Solar Collectors In: Solar Energy: The State of the Art*, edn. Original, James Ltd, United Kingdom, pp. 166-168. 2001.

[12] American Society of Heating, Refrigerating And Air Conditioning Engineers. *ASHRAE Handbook Fundamentals*; Atlanta, 2009.

[13] Miroshnichenko IV, Sheremet MA. Turbulent natural convection heat transfer in rectangular enclosures using experimental and numerical approaches: A review. *Renewable and Sustainable Energy Reviews* 2018; 82:40–59.

[14] Jongen T. *Simulation and Modeling of Turbulent Incompressible Flows*. PhD Thesis, École polytechnique fédérale de Lausanne, Switzerland; 1992.

[15] Kader BA. Temperature and concentration profiles in fully turbulent boundary layers. *International Journal of Heat and Mass Transfer* 1981; 24(9):1541–4.

[16] Watmuff J, Charters W, Proctor D. Solar and wind induced external coefficients - *Solar collectors* 1977; Jun 1;56.

[17] Çengel YA. *Heat transfer : a practical approach*: Boston Mcgraw-Hill; 2006.

[18] Lança M, Gomes J, Cabral D. Thermal performance of three concentrating collectors with bifacial photovoltaic cells part I – Experimental and computational fluid dynamics study. *Proceedings of the Institution of Mechanical Engineers, Part A: Journal of Power and Energy.* 2023;0(0).